



Article

# Effect of Polynorbornene on Physico-Mechanical, Dynamic, and Dielectric Properties of Vulcanizates Based on Isoprene, $\alpha$ -Methylstyrene-Butadiene, and Nitrile-Butadiene Rubbers for Rail Fasteners Pads

Evgeniy N. Egorov <sup>1,\*</sup> , Evgeniia V. Salomatina <sup>2</sup> , Vladislav R. Vassilyev <sup>3</sup>, Alexander G. Bannov <sup>4,\*</sup> and Sergey I. Sandalov <sup>5</sup>

- <sup>1</sup> Department of Physical Chemistry and Macromolecular Compounds, Faculty of Chemistry and Pharmacy, Chuvash State University Named after I.N. Ulyanov, 15 Moskovsky Prosp., 428015 Cheboksary, Russia
- <sup>2</sup> Department of Macromolecular Compounds and Colloidal Chemistry, Faculty of Chemistry, N.I. Lobachevsky State University of Nizhny Novgorod, 23 Gagarin Avenue, 603022 Nizhny Novgorod, Russia; salomatina\_ev@mail.ru
- <sup>3</sup> Department of Solid State Physics, Institute of Physics, Kazan Federal University, 18 Kremlyovskaya Str., 420008 Kazan, Russia; vlad.v99@bk.ru
- <sup>4</sup> Department of Chemistry and Chemical Technology, Faculty of Mechanics and Technology, Novosibirsk State Technical University, 20 K. Marx Ave., 630073 Novosibirsk, Russia
- <sup>5</sup> Cheboksary Production Association Named after V. I. Chapaev, 1 St. Socialist, 428006 Cheboksary, Russia; sandalov-1963@yandex.ru
- \* Correspondence: enegorov@mail.ru (E.N.E.); bannov.alexander@gmail.com (A.G.B.)



**Citation:** Egorov, E.N.; Salomatina, E.V.; Vassilyev, V.R.; Bannov, A.G.; Sandalov, S.I. Effect of Polynorbornene on Physico-Mechanical, Dynamic, and Dielectric Properties of Vulcanizates Based on Isoprene,  $\alpha$ -Methylstyrene-Butadiene, and Nitrile-Butadiene Rubbers for Rail Fasteners Pads. *J. Compos. Sci.* **2023**, *7*, 334. <https://doi.org/10.3390/jcs7080334>

Academic Editor:  
Francesco Tornabene

Received: 26 July 2023

Revised: 9 August 2023

Accepted: 14 August 2023

Published: 16 August 2023



**Copyright:** © 2023 by the authors. Licensee MDPI, Basel, Switzerland. This article is an open access article distributed under the terms and conditions of the Creative Commons Attribution (CC BY) license (<https://creativecommons.org/licenses/by/4.0/>).

**Abstract:** The article studies the effect of polynorbornene (PNB) in the composition of PNB with Norman 747 LV plasticizer (RC) on the curing characteristics of the rubber compound and the physico-mechanical, dynamic, dielectric properties and the thermal behavior of vulcanizates based on a combination of isoprene,  $\alpha$ -methylstyrene-butadiene, and nitrile-butadiene rubbers. It is shown that vulcanizates containing PNB in the composition of the RC had lower conditional tensile strength, hardness, and tear resistance compared to the vulcanizate of the base version of the rubber compound. Studies of dynamic mechanical analysis indicate that an increase in the content of RC, and hence PNB, in the rubber compound contributes to an increase in the mechanical loss factor ( $\tan\delta$ ) and a decrease in the storage modulus of vulcanizates. It was found that vulcanized rubber, containing 24.0 parts per hundred of rubber (phr) (8.98 wt. %) PNB as part of the RC, is characterized by stable physico-mechanical, improved vibration-absorbing properties, as well as increased dielectric parameters. This rubber compound can be used as a base for rail fasteners for railroad tracks.

**Keywords:** rubber compound; polynorbornene; curing characteristics; crosslink density; physico-mechanical properties; dynamic mechanical analysis; dielectric properties; thermal behavior; rail fastening gaskets

## 1. Introduction

Railways create increased levels of vibration and noise during operation caused by the interaction of the rolling stock and the railway track [1–7]. The noise generated during the operation of railway transport has a negative impact on human health [8–14]. To solve this problem, rubber gaskets for rail fastenings are used [15–19]. These gaskets are made using directional functional ingredients to improve the vibration-damping (noise-absorbing) properties of the rubber. Increasing the vibration-damping properties of rubber is achieved by selecting the optimal polymer base. The modification of rubbers and their combination with polymers of a different nature and structure is one of the promising ways to create composite materials with improved vibration-damping properties [20–22]. These properties increase when various ingredients are introduced into the rubber composition,

which leads to the irreversible conversion of vibration energy into heat [23,24]. One of these ingredients is polynorbornene (PNB), a product of the metathesis polymerization of norbornene (bicyclo-[2,2,1]-hept-2-ene) [25–28].

Industrial polynorbornene, obtained using a  $\text{RuCl}_3$ -based catalyst in an alcohol medium, has found an application for the manufacturing of rubbers with unique vibration and sound-dampening characteristics. In the late 1970s, “CdF Chimie” launched the production of this polymer under the trade name Norsorex<sup>®</sup> [29,30]. The commercial product Norsorex<sup>®</sup> has a high content of trans double bonds (i.e., 90%) [31], a molecular weight of about  $3 \times 10^6$ , and a glass transition temperature ( $T_g$ ) ranging from 35 to 45 °C [32]. The relatively high glass transition temperature of Norsorex<sup>®</sup> contributes to its excellent damping properties under shock, vibration, and sound insulation [33]. At room temperature, PNB is a solid product and exhibits rubber-like properties when plasticizers are added [31,34,35]. In addition, PNB has good physical characteristics, such as high thermal stability, low moisture absorption, and low dielectric constant, which makes it attractive for electronic applications [36].

Due to its low polarity and high molecular weight, Norsorex<sup>®</sup> can absorb hydrocarbons up to 10 times its dry weight, forming a gel that retains good mechanical properties. Accordingly, it has found some use in oil spill responses. In addition, hydrocarbon plasticizers can be added to obtain formulations containing more than 400 phr of the plasticizer, which makes it possible to obtain polynorbornene compositions with  $T_g$  down to  $-60$  °C [33]. Another advantage of Norsorex<sup>®</sup> is that compositions based on it can have high friction coefficients in a wide temperature range and have a good ability to absorb vibrational energy [31].

Several works have been devoted to the study of PNB in various polymer composite materials, including vulcanized rubbers. Thus, in [34], the influence of polynorbornene rubber (PNR) in the composition of ethylene propylene diene monomer rubber EPDM 2650 at different ratios on the dynamic characteristics of vulcanizates was considered. Dynamic mechanical analysis (DMA) showed that the temperature range of effective damping ( $\tan\delta \geq 0.3$ ) of vulcanized PNR was about 113 °C, and this range decreases as the EPDM content in the mixture increases. The PNR/EPDM vulcanizate at a ratio of 25/75 phr has a  $\tan\delta$  value at the point of maximum ( $\tan\delta_{\max} = 1.62$ ) at a temperature of  $-34$  °C. The work [37] describes the damping properties of rubber based on nitrile-butadiene rubber (NBR) and PNB (Norsorex<sup>®</sup>). The DMA results showed that Norsorex at 30 phr in 70 phr NBR significantly improved the damping characteristics of the vulcanizate based on them. Vulcanized rubber based on the combination of NBR, Norsorex<sup>®</sup> = 70:30 phr possessed the highest  $\tan\delta_{\max}$  of 0.788 at 19.7 °C.

Norsorex is used for damping elements, for example, for railway, automotive, and acoustic systems, and as a tread compound for tires and personal protective equipment. Often Norsorex<sup>®</sup> is also used in blends with other rubbers to optimize their properties for special applications [31]. In this regard, it is of interest to study the effect of PNB on the curing characteristics of the rubber compound, physico-mechanical, dynamic, and dielectric properties of vulcanized rubber based on isoprene SKI-3,  $\alpha$ -methylstyrene-butadiene SKMS-30ARK and nitrile-butadiene SKN 2655 rubbers with sulfur vulcanizing system used for the manufacture of gaskets for rail fasteners of the railway track.

## 2. Experimental

### 2.1. Materials

The following rubbers and ingredients served as the basis for the studied rubber mixture: isoprene rubber SKI-3 with Mooney viscosity  $ML_{1+4}$  (100 °C) 76–85 (Sintez-Kauchuk, Sterlitamak, Russia),  $\alpha$ -methylstyrene-butadiene rubber SKMS-30ARK with the content of binder  $\alpha$ -methylstyrene 22–25 wt. % and Mooney viscosity  $ML_{1+4}$  (100 °C) 46–57 (Omskii Kauchuk, Omsk, Russia), nitrile-butadiene rubber NBR 2655 with a mass fraction of acrylic acid nitrile 27–30 wt. %, Mooney viscosity  $ML_{1+4}$  (100 °C) 52–58 (Sibur, Moscow, Russia); curing (vulcanizing) agents–sulfur (Kaspiygaz, Astrakhan, Russia),

N,N'-dithiodimorpholine (DTDM) (KurskKhimProm, Kursk, Russia); vulcanization accelerators–N-cyclohexyl-2-benzothiazolesulfenamide Vulkacit CZ/C (Lanxess, Cologne, Germany) (CBS), tetramethylthiuram disulfide (TMTD) (Himstar, Volzhsky, Russia); vulcanization activators–zinc oxide (ZnO) (Empils-zinc, Rostov-on-don, Russia), stearic acid (RossPolymer, Moscow, Russia); antioxidants–N-isopropyl-N'-phenyl-p-phenylenediamine Vulkanox 4010 NA/LG (Lanxess, Germany) (IPPD), poly(1,2-dihydro-2,2,4-trimethylquinoline) acetanil N (TMQ) (Khimprom, Novocheboksarsk, Russia), wax ZV-P (KhimAvangard, Dzerzhinsk, Russia); fillers–silicon dioxide Zeosil 1165 MP with a specific surface area of 140–180 m<sup>2</sup>/g (Solvay, Brussels, Belgium), carbon black N 220 (Nizhnekamsktehuglerod, Nizhnekamsk, Russia) and carbon black P 514 (Ivanovskii Tekhuglerod i Rezina, Ivanovo, Russia) with a specific surface area of 104–118 and 50–57 m<sup>2</sup>/g, respectively, kaolin with a specific surface area of 10–24 m<sup>2</sup>/g (Plast-Rifey, Chelyabinsk Oblast, Russia); modifier–Hepsol KhKP (copolymer based on hexachloro-*para*-xylene and chlorinated paraffin) (Kaustik, Volgograd, Russia); softener–rosin (Orgsintez, Nizhny Novgorod, Russia); scorch retarder–N-nitrosodiphenylamine (RossPolymer, Moscow, Russia); PNB brand Norsorex NS with a particle size of 300–400 μm, a bulk density of 0.35–0.40 g/cm<sup>3</sup> (Astron Industriebeteiligungs GmbH, Wien, Austria); plasticizer, the mixture of aromatic hydrocarbons, Norman 747 LV with kinematic viscosity at 40 °C 14.3 cSt, density at 20 °C 1037 kg/m<sup>3</sup>, refractive index at 20 °C 1.63 (Orgkhim, Nizhny Novgorod, Russia).

## 2.2. Preparation of the Samples

The direct introduction of powdered PNB into the rubber compound is not possible due to its poor combination with the elastomeric matrix. To eliminate this drawback, a rubber-like composition (RC) was developed. The production of RC was carried out in two stages. First, PNB was mixed with plasticizer Norman 747 LV at a mass ratio of PNB:Norman 747 LV = 1.0:1.5, at a temperature of 70 °C for 1.5 h. Then the resulting swollen product was subjected to rolling on a BH 2102 roller (650 300/300) with constant undercutting of the stock of composition formed on the front roll of the rollers on both sides of this roll for 20 min at a temperature of the rolls of 50–60 °C. After rolling, a RC was obtained, which was cut off from the front roll in the form of a sheet. Subsequently, the RC was introduced into the studied rubber mixture in various amounts.

The first (basic) version (PB-1) of the rubber compound was prepared without the use of RC. Its second–fifth variants (PB-2 ÷ PB-5) were prepared with additives of 15.0, 30.0, 45.0, and 60.0 phr. The RC corresponds to the content of PNB in quantities of 6.0, 12.0, 18.0, 24.0 phr (2.70, 5.06, 7.14, 8.98 wt. %) and included the RC Norman 747 LV in quantities of 9.0; 18.0; 27.0 and 36.0 phr. The rubber compounds investigated are shown in Table 1. The rubber compound was prepared by mixing a combination of rubbers SKI-3, SKMS-30ARK, and NBR 2655 with the ingredients given in Table 1 on laboratory rollers LB 320 160/160 under the most identical conditions; the temperature of the surface of the rollers was 60–70 °C, the mixing cycle duration was 25 min.

The standard samples of all rubber compounds for determining physico-mechanical parameters were vulcanized at 143 °C, a pressure of 17.6 MPa for 20 min in a P-V-100-3RT-2-PCD type vulcanizing press.

## 2.3. Curing Characteristics

The curing properties of the rubber compound were studied on an MDR 3000 Basic rheometer (Mon Tech Co., Buchen, Germany) at 143 °C for 40 min in accordance with ASTM D5289.

**Table 1.** Rubber compounds investigated.

Rubbers and Additives	Content (phr *) for Various Samples				
	PB-1	PB-2	PB-3	PB-4	PB-5
SKI-3	50.0	50.0	50.0	50.0	50.0
SKMS-30ARK	30.0	30.0	30.0	30.0	30.0
NBR 2655	20.0	20.0	20.0	20.0	20.0
Curing agents	2.8	2.8	2.8	2.8	2.8
Vulcanization accelerators	2.3	2.3	2.3	2.3	2.3
Vulcanization activators	7.0	7.0	7.0	7.0	7.0
Antioxidants	4.0	4.0	4.0	4.0	4.0
Fillers	88.0	88.0	88.0	88.0	88.0
Modifier	1.0	1.0	1.0	1.0	1.0
Softener	1.0	1.0	1.0	1.0	1.0
Scorch retarder	1.0	1.0	1.0	1.0	1.0
RC	–	15.0	30.0	45.0	60.0

\* Parts per hundred parts of rubber.

### 2.4. Crosslink Density

Most often, the crosslink density is determined from the data of the equilibrium swelling of the vulcanizate. Rectangular samples of vulcanizates with dimensions of 25 × 7 × 2 mm were cut out from the central part of the rubber plate and immersed in toluene in a closed container for 72 h at room temperature. After reaching the equilibrium degree of swelling, the sample was removed from the solvent (toluene), quickly dried with filter paper, and weighed. Then the swollen samples were placed in an oven and dried at 60 °C for 24 h to remove the solvent. The dried samples of vulcanizates were weighed.

There is the following relationship, described by the Flory–Rehner equation, between the average molecular weight of a segment of the molecular chain ( $M_c$ ), enclosed between two crosslinks, and the volume fraction of rubber in the swollen vulcanizate ( $v_r$ ) Equation (1) [38]:

$$M_c = - \frac{\rho_r V_s (\sqrt[3]{v_r} - \frac{v_r}{2})}{\ln(1 - v_r) + v_r + \chi v_r^2} \tag{1}$$

where  $\chi$  describes the Flory–Huggins polymer-solvent interaction parameter,  $v_s$  is the molar volume of the solvent used (i.e., 106.27 cm<sup>3</sup>/mol for toluene [39]), and  $\rho_r$  (g/cm<sup>3</sup>) is the density of rubber.

$v_r$  is determined by Equation (2):

$$v_r = \frac{1}{\left[ 1 + \left( \frac{W_s - W_d}{W_d} \right) \right] \frac{\rho_r}{\rho_s}} \tag{2}$$

where  $W_s$  is the weight of the swollen sample,  $W_d$  is the weight of the sample dried after swelling,  $\rho_r$  and  $\rho_s$  represent the density of the rubber and solvent, respectively [40,41].  $\rho(\text{SKI-3}) = 0.92 \text{ g/cm}^3$ ;  $\rho(\text{SKMS-30ARK}) = 0.93 \text{ g/cm}^3$ ;  $\rho(\text{NBR 2655}) = 0.96 \text{ g/cm}^3$ . Using the additivity rule, we get  $\rho(\text{SKI-3-SKMS-30ARK-NBR 2655}) = 0.93 \text{ g/cm}^3$ . The solvent density was  $\rho(\text{toluene}) = 0.8669 \text{ g/cm}^3$ .

A widely used equation to calculate  $\chi$ , based on the Hildebrand solubility parameters is

$$\chi = \beta + \frac{V_s}{RT} (\delta_r - \delta_s)^2 \tag{3}$$

where  $\delta_r$  and  $\delta_s$  is the solubility parameters for rubber and solvent (18.2 (J/cm<sup>3</sup>)<sup>1/2</sup> for toluene [42]), respectively, R the molar gas constant (8.314 J/(mol·K)), and T the absolute temperature (293.15 K),  $\beta$  is the entropic contribution ( $\beta = 0.34$  [39]).

The solubility parameter of rubbers was calculated using the method of group contributions, which is described in [43]. The values of the rubber solubility parameter

calculated by the method of group contributions are  $\delta(\text{SKI-3}) = 16.5 \text{ (J/cm}^3\text{)}^{1/2}$ ;  $\delta(\text{SKMS-30ARK}) = 17.2 \text{ (J/cm}^3\text{)}^{1/2}$ ;  $\delta(\text{NBR 2655}) = 19.5 \text{ (J/cm}^3\text{)}^{1/2}$ . Substituting the obtained values of the solubility parameter into Equation (3), the Flory–Huggins interaction parameter  $\chi$  was calculated for each rubber:  $\chi(\text{SKI-3}) = 0.466$ ;  $\chi(\text{SKMS-30ARK}) = 0.384$ ;  $\chi(\text{NBR 2655}) = 0.414$ . Applying the additivity rule for the SKI-3–SKMS-30ARK–NBR 2655 system, we obtain the value  $\chi = 0.431$ .

The crosslink density  $\nu_c$  (mol/cm<sup>3</sup>) is calculated using Equation (4) [44,45]:

$$\nu_c = \frac{\rho_r}{2M_c} \quad (4)$$

### 2.5. Differential Scanning Calorimetry

The DSC study of PNB samples and RC composition was carried out on a DSC 204 F1 Phoenix differential scanning calorimeter (Netzsch, Selb, Germany) in the temperature range from  $-120$  to  $150$  °C. Scanning was performed at a rate of  $20$  °C/min with liquid nitrogen cooling in an argon atmosphere using a standard aluminum crucible with a lid. The weight of the samples was  $10$ – $11$  mg. An empty aluminum crucible served as a reference sample.

### 2.6. Thermogravimetric Analysis (TGA)

TGA of the samples was carried out on a synchronous thermal analyzer STA 409 PC (Netzsch, Germany) in an inert argon atmosphere in the temperature range of  $30$ – $550$  °C (for PNB samples and RC) and  $30$ – $700$  °C (for vulcanizate samples) at a heating rate of  $10$  °C/min. The samples were placed in an open ceramic crucible ( $\text{Al}_2\text{O}_3$ ). The weight of the samples was  $5$ – $6$  mg.

### 2.7. Physico-Mechanical Properties

Modulus stress at 100% elongation, tensile strength, and elongation at break of vulcanizates (samples in the amount of five double-sided blades with a thickness of  $(2.0 \pm 0.2)$  mm for each version of vulcanizate) were determined in accordance with ASTM D412 using tensile testing machine REM-5-M-1-2 (Metrotest, Moscow, Russia) at a gripper speed of  $500$  mm/min. The mean of these indicators of five tested samples for each variant of the vulcanizate was taken as the test result.

Shore A hardness was determined using a TVR-A hardness tester (Vostok-7, Moscow, Russia) on one sample in the form of a washer with parallel planes with a diameter of  $50$  mm and a thickness of  $8$  mm for each version of the vulcanizate according to ASTM D2240-15. Hardness was measured at three points in different places of the sample. The test result was taken as the arithmetic mean of all measurements, rounded up to a whole number.

The tear resistance was determined on five arcuate samples with a thickness of  $(2.0 \pm 0.2)$  mm for each variant of the vulcanizate in accordance with ASTM D624 using REM-5-M-1-2 tensile testing machine at a gripper speed of  $500$  mm/min. The arithmetic mean of five tested samples for each variant of the vulcanizate was taken as the test result.

Relative static compression set (RSC) in air was determined on three samples in the form of cylinders with a diameter and height of  $(9.8 \pm 0.1)$  mm for each vulcanizate according to ASTM D395-18. The test result was taken as the arithmetic mean of three tested samples for each version of the vulcanizate.

Abrasion was determined on six (three pairs) samples in the form of square plates with a side of  $(20.0 \pm 0.5)$  mm and a thickness of  $(8.0 \pm 0.5)$  mm according to ASTM D5963-22. The test result was taken as the arithmetic mean of three values of indicators that differ from the average by no more than 10% for each variant of the vulcanizate.

### 2.8. Dynamic Mechanical Analysis (DMA)

Dynamic parameters (storage modulus, mechanical loss factor ( $\tan\delta$ )) of vulcanizates (samples were  $30 \times 10 \times 2$  mm in dimensions) were studied on a Netzsch DMA 242 E

Artemis dynamic mechanical analyzer (Netzsch, Germany) in the temperature range from  $-90$  to  $90$  °C at a heating rate  $2$  °C/min; oscillation frequency was  $1$  Hz, amplitude was  $40$   $\mu\text{m}$ , force acting on the sample was  $12$  N. The measurements were carried out using a three-point bending deformation mode.

### 2.9. Dielectric Properties

The temperature dependence of electrical properties of polymer samples (thickness was  $2.0$ – $2.1$  mm) was recorded in the temperature range from  $-70$  to  $100$  °C at a frequency of  $1$  kHz, every  $2$  °C using E7-20 immittance meter (MNIPI, Minsk, Belarus). The setup consisted of a measuring cell with a sample placed in a Dewar flask filled with nitrogen and connected to an E7-20 RLC meter and a V7-78 universal voltmeter functioning as a precision thermometer. A laboratory-adjustable autotransformer was used to smoothly control the temperature change. The sample in the measuring cell was placed in a “cool” furnace, the neck of which was placed in a Dewar vessel. Thus, the samples were first heated to  $100$  °C. Then, the autotransformer was switched to the evaporator, and the samples were cooled to  $-70$  °C with evaporating nitrogen. The error in measuring the dielectric loss tangent was  $\pm 2\%$ , and the accuracy of temperature control was  $\pm 0.1$  °C.

## 3. Results and Discussion

### 3.1. Curing Characteristics and Crosslink Density

Figure 1 shows curing (vulcanization) curves for various types of rubber compounds at a temperature of  $143$  °C.

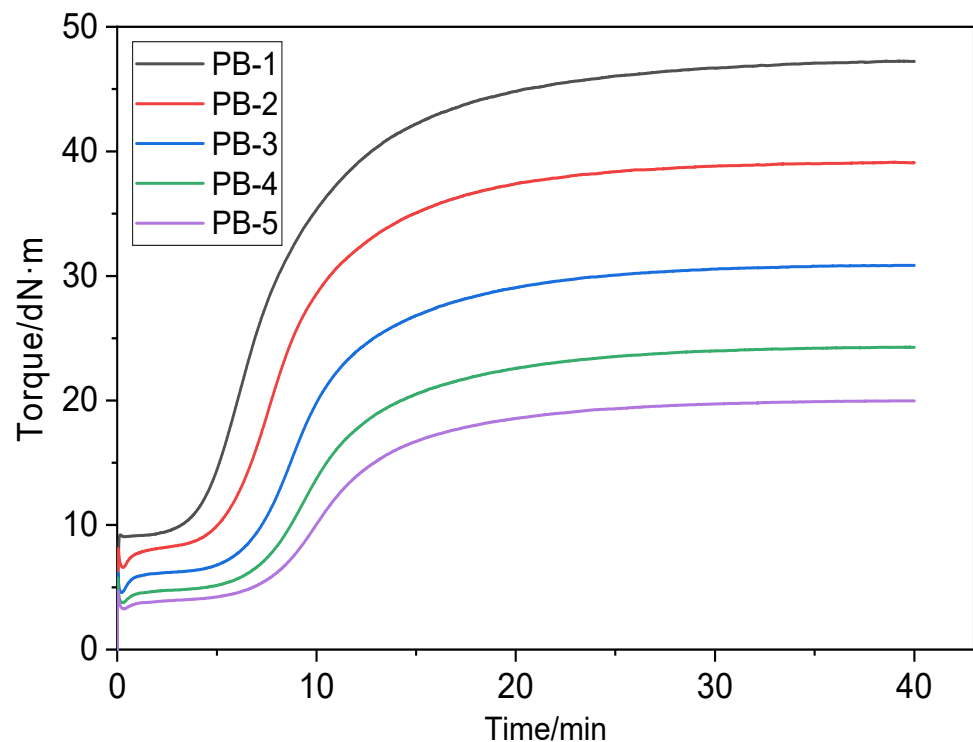


**Figure 1.** Curing curves for various rubber compounds at  $143$  °C.

Based on these curves, the cure characteristics were determined and are shown in Table 2.

**Table 2.** Curing (vulcanization) characteristics of rubber compound.

Characteristics	Samples				
	PB-1	PB-2	PB-3	PB-4	PB-5
$M_L$ , dN·m	10.21	7.79	5.62	4.58	3.92
$M_H$ , dN·m	47.51	39.33	31.02	24.40	20.07
$\Delta M$ , dN·m	37.30	30.17	25.40	19.82	16.15
$t_s$ , min	2.94	3.70	4.58	6.15	7.14
$t_{90}$ , min	16.12	16.22	17.58	18.73	18.90

Notation:  $M_H$  is the maximum torque;  $M_L$  is the minimum torque;  $\Delta M$  is the difference between maximum and minimum torque;  $t_s$  is the curing scorch time;  $t_{90}$  is the optimum curing time.

As can be seen from Table 2, a decrease in the maximum  $M_H$  and minimum  $M_L$  torques and their difference ( $\Delta M$ ) was observed with an increase in the RC content in the rubber compound compared to the base (PB-1 sample) version. This, apparently, is due to an increase in the amount of Norman 747 LV plasticizer contained in the RC. At the same time, there is an increase in the curing scorch time and optimum curing time of the rubber compound, including the RC, which contributes to the improvement of its technological properties (processability by calendaring methods, i.e., a technological operation for manufacturing blanks of rubber compound for vulcanization, followed by the production of finished rail pads). It is known [46,47] that the value of  $\Delta M$  is directly proportional to the degree of crosslinking of the vulcanizate. In this regard, the PB-5 vulcanizate containing 60.0 phr RC should possess the lowest degree of crosslinking and, therefore, is characterized by lower strength properties compared to rubber which does not contain RC.

Table 3 shows the data on the density of crosslinking of vulcanizates of the studied rubber compound.

**Table 3.** Crosslink density of vulcanizates.

Characteristics	Samples				
	PB-1	PB-2	PB-3	PB-4	PB-5
$\nu_r$	0.409 ± 0.001	0.381 ± 0.001	0.342 ± 0.001	0.328 ± 0.001	0.306 ± 0.001
$M_c \times 10^{-3}$ , g/mol	1.186 ± 0.009	1.460 ± 0.006	1.999 ± 0.016	2.239 ± 0.010	2.722 ± 0.012
$\nu_c \times 10^4$ , mol/cm <sup>3</sup>	3.922 ± 0.030	3.189 ± 0.012	2.328 ± 0.019	2.079 ± 0.009	1.709 ± 0.007

Notation:  $\nu_r$  is the volume fraction of rubber in the swollen vulcanizate;  $M_c$  is the average molecular weight of a segment of the molecular chain;  $\nu_c$  is the crosslink density.

Table 3 data confirm the above assumption that the value of  $\Delta M$  is directly proportional to the crosslink density of vulcanizate  $\nu_c$ . The decrease in the crosslink density  $\nu_c$  of the vulcanizate was observed when increasing the RC content in the rubber compound that is caused by an increase in the fraction of Norman 747 LV plasticizer contained in the RC and, consequently, due to a decrease in the intermolecular interaction of rubber macromolecules. As expected, the PB-5 vulcanizate is characterized by the lowest crosslink density. This is due to the high content of the Norman 747 LV plasticizer in the PB-5 vulcanizate, which loosens the spatial vulcanization mesh and leads to an increase in the mobility of rubber macromolecules.

### 3.2. Thermal Analysis

The estimation of glass transition temperature  $T_g$  of PNB and the RC was estimated using the DSC method. Figure 2 shows the DSC curves of PNB and RC.

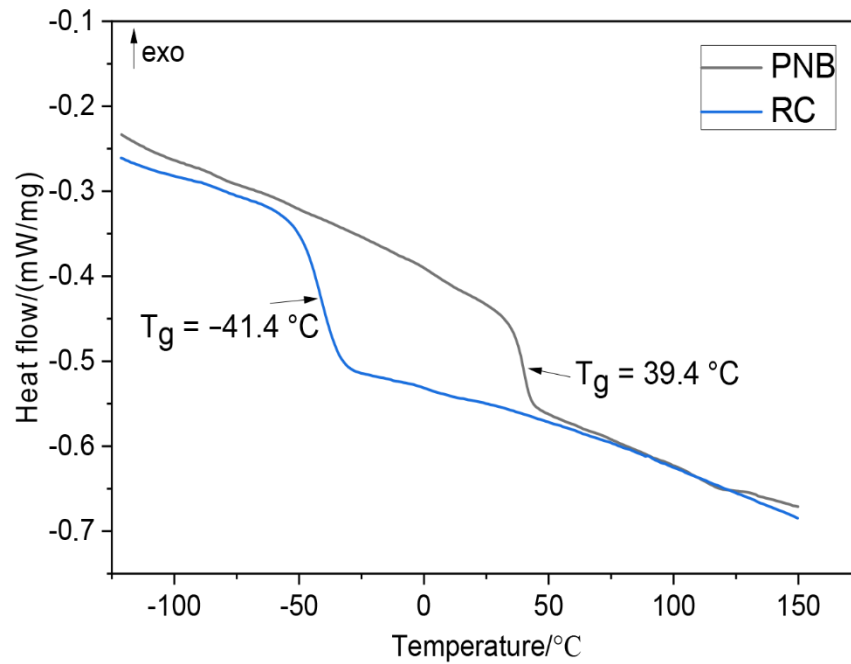


Figure 2. DSC curves of PNB and RC.

As can be seen from Figure 2, the glass transition temperature of PNB was 39.4 °C. The introduction of Norman 747 LV plasticizer into powdered PNB led to a shift of the endothermic inflection on the DSC curve to lower temperatures. The rubber-like composition had a glass transition temperature of  $T_g = -41.4$  °C.

We also studied the thermal stability of PNB and RC by TGA method (Figure 3).

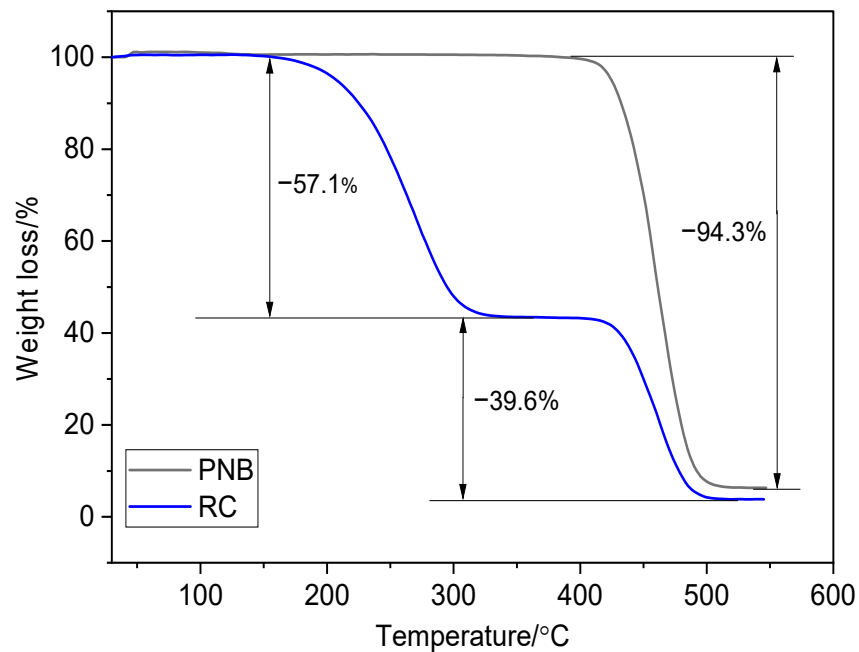


Figure 3. TGA curves of PNB and RC.

Figure 3 displays that TGA for PNB shows continuous absorption of heat up to 385 °C without weight loss (onset of weight loss at 433.7 °C). Sample decomposition occurs at 497 °C. RC is characterized by two-stage decomposition: the beginning of mass loss for the first stage is observed at a temperature of 217.6 °C, which is probably associated with the onset of evaporation of the plasticizer Norman 747 LV. When the temperature reaches

310 °C, the plasticizer contained in the RC completely evaporates. The onset of weight loss in the second stage of RC decomposition is characterized at a temperature of 432 °C, which is obviously associated with the onset of degradation of PNB macromolecules. At a temperature of 486 °C, decomposition of the RC is observed.

### 3.3. Physico-Mechanical Properties

The results of the physico-mechanical properties of vulcanizates are given in Table 4.

**Table 4.** Physico-mechanical properties of vulcanizates.

Characteristics	Samples				
	PB-1	PB-2	PB-3	PB-4	PB-5
$f_{100}$ , MPa	9.0 ± 0.3	7.1 ± 0.2	6.4 ± 0.2	5.2 ± 0.2	4.8 ± 0.2
$f_p$ , MPa	18.4 ± 0.6	17.9 ± 0.6	16.8 ± 0.6	16.3 ± 0.5	15.9 ± 0.5
$\epsilon_p$ , %	240 ± 9	310 ± 12	370 ± 14	410 ± 16	430 ± 17
$H$ , a.u. Shore A	85 ± 1	83 ± 1	80 ± 1	75 ± 1	70 ± 1
$B$ , kN·m <sup>-1</sup>	59 ± 2	56 ± 2	51 ± 2	49 ± 2	47 ± 2
RSC at 30% compression(100 °C, 24 h), %	31.9 ± 0.7	32.8 ± 0.6	32.6 ± 0.6	32.2 ± 0.7	33.9 ± 0.7
$\alpha$ , m <sup>3</sup> ·TJ <sup>-1</sup>	51.2 ± 2.5	53.9 ± 2.6	56.6 ± 2.8	59.1 ± 2.9	63.7 ± 3.1

Notation:  $f_{100}$  is the modulus stress at 100% elongation;  $f_p$  is the tensile strength;  $\epsilon_p$  is the elongation at break;  $H$  is the hardness;  $B$  is the tear resistance; RSC is the relative static compression set;  $\alpha$  is the abrasion.

Data in Table 4 shows that vulcanizes containing RC had lower modulus stress at 100%, tensile strength, hardness, and tear resistance compared to the vulcanizate of the PB-1 sample (for the vulcanizate PB-5, compared with the first PB-1, there is a decrease in the modulus stress at 100% elongation by 46.7%, tensile strength by 13.6%, hardness by 17.6% and tear resistance by 20.4%). This is probably caused by the fact that the Norman 747 LV plasticizer will be adsorbed on the surface of the filler and protect its surface from interaction with rubber macromolecules. In this case, there is an increase in the elongation at break, the RSC, and the abrasion of the vulcanizates (the PB-5 vulcanizate is characterized by an increase in the elongation at break by 79.2%, the RSC by 6.3%, and the abrasion by 24.4% compared to the vulcanizate that does not contain the RC composition). This is due to a decrease in the viscosity of the rubber compound with an increase in the content of the RC in it, and, hence, the concentration of the plasticizer in it, which is confirmed by the minimum torque  $M_L$  indirectly characterizes the viscosity of the rubber compound. A decrease in the viscosity of the rubber compound contributes to an increase in the segmental mobility of rubber macromolecules, which leads to an increase in elongation at break, RSC, and rubber abrasion.

It should be noted that the introduction of a plasticizer molecularly distributed between the polymer chains into the composition of the rubber compound leads to an increase in the free volume proportional to the amount of the plasticizer. Thus, a decrease in strength characteristics with an increase in the content of plasticizer is a natural effect.

### 3.4. Dynamic Mechanical Properties

A quantitative measure for assessing the dynamic (vibration-absorbing, damping) properties of polymer materials, including vulcanized rubbers, are the mechanical loss factor ( $\tan\delta$ ) and the storage modulus ( $E'$ ) [48,49]. In connection with this, the values of  $\tan\delta$  and  $E'$  of the vulcanizates were determined by the DMA. The glass transition temperature  $T_g$  was determined as the temperature of the maximum temperature dependence of  $\tan\delta$ . Figures 4 and 5 show the curves of the temperature dependences of  $E'$  and  $\tan\delta$  for the vulcanizates of the rubber compound. Table 5 shows the dynamic parameters of the investigated vulcanizates.

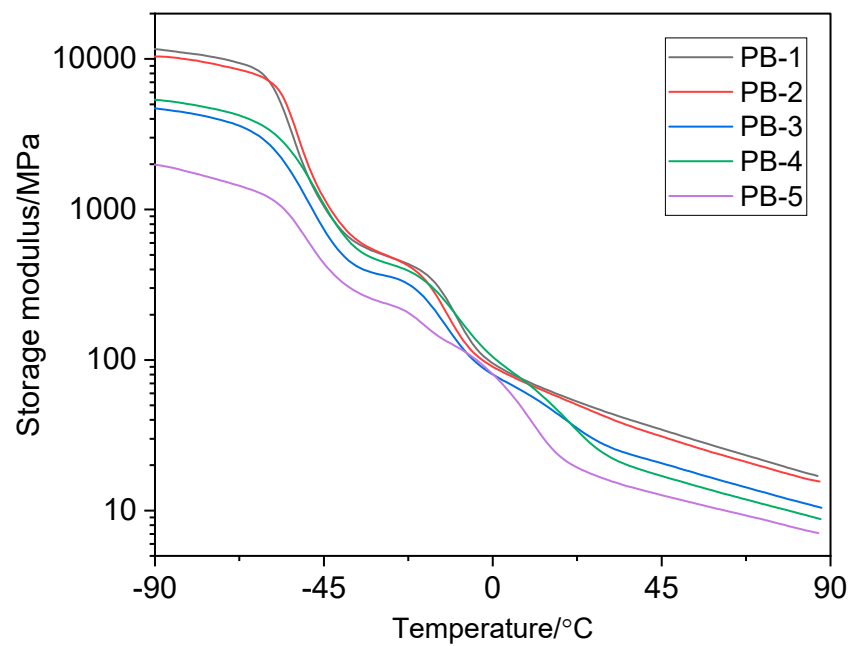


Figure 4. Temperature dependences on the storage modulus of vulcanizates of different rubber compounds.

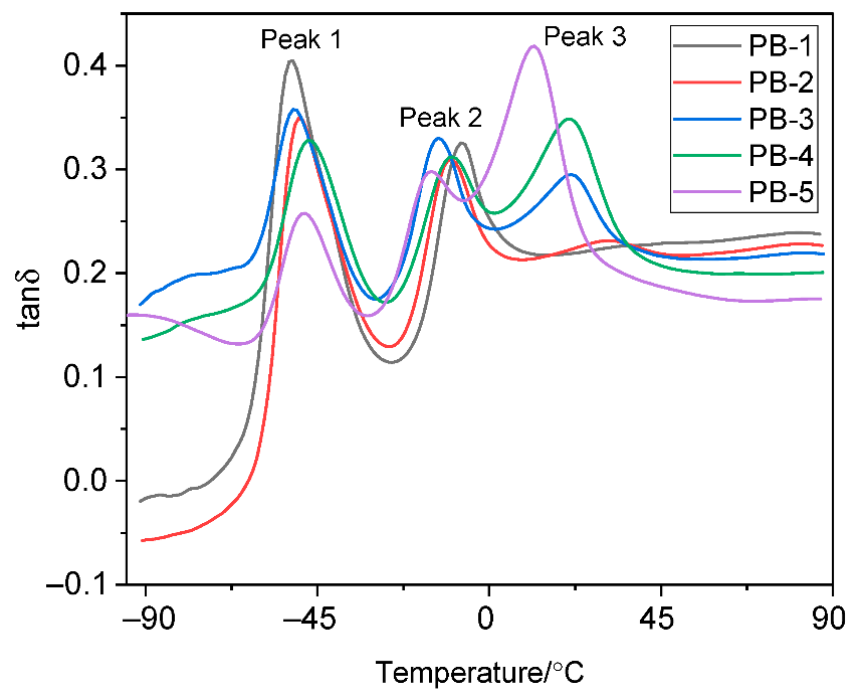


Figure 5. Temperature dependences of the  $\tan\delta$  of vulcanizates of rubber compounds.

Table 5. Dynamic properties of vulcanizates.

Sample	Peak 1		Peak 2		Peak 3	
	$\tan\delta_{\max}$	$T_{g'} \text{ } ^\circ\text{C}$	$\tan\delta_{\max}$	$T_{g'} \text{ } ^\circ\text{C}$	$\tan\delta_{\max}$	$T_{g'} \text{ } ^\circ\text{C}$
PB-1	0.405	-51.8	0.326	-7.0	-	-
PB-2	0.350	-49.7	0.310	-10.1	0.231	31.3
PB-3	0.358	-51.1	0.330	-13.3	0.295	21.4
PB-4	0.328	-47.2	0.312	-9.7	0.349	20.8
PB-5	0.258	-48.2	0.298	-15.2	0.419	11.8

As can be seen from Figure 4, an increase in the content of RC and, consequently, PNB in the composition of the rubber mixture contributes to a decrease in the elasticity modulus of the vulcanizate in the glassy state. Moreover, the PB-5 vulcanizate had the lowest value of  $E'$  in the entire temperature range of measurements.

As can be seen from Figure 5, the temperature dependence of  $\tan\delta$  in the studied temperature range for vulcanizates has a multimodal character. For the vulcanizate of the basic version PB-1, a bimodal form of the temperature dependence of  $\tan\delta$  is observed. The peak at  $-51.8\text{ }^\circ\text{C}$  (peak 1) with  $\tan\delta_{\max} = 0.405$  (Table 5) refers to the “joint” phase of isoprene and butadiene- $\alpha$ -methylstyrene rubbers, and the peak at  $-7.0\text{ }^\circ\text{C}$  (peak 2) to the phase of nitrile-butadiene rubber, which indicates the thermodynamic incompatibility of SKN 2655 with SKMS-30ARK and SKI-3 rubbers. Vulcanizates containing PNB had a trimodal nature of temperature dependence of  $\tan\delta$ , i.e., peaks in the temperature range from  $-51.1$  to  $-47.2\text{ }^\circ\text{C}$  belong to the SKI-3 and SKMS-30ARK phases, peaks in the temperature range from  $-15.2$  to  $-9.7\text{ }^\circ\text{C}$  to the SKN 2655 phase. The peaks that appeared in the temperature range  $11.8$ – $31.3\text{ }^\circ\text{C}$  belong to the PNB phase. From Figure 5, it can be seen that the peaks in the region of positive temperatures shift towards lower values with an increase in the content of RC and, consequently, PNB in the composition of the rubber mixture. In this case, a decrease in the glass transition temperature of the PNB phase is observed due to an increase in the proportion of Norman 747 LV plasticizer contained in the RC.

It is known [50–55] that the sound-absorbing (vibration-damping) properties increase with an increase in the mechanical loss tangent of polymers (vulcanized rubbers). The highest value of  $\tan\delta$  and the lowest value of  $E'$ , and, consequently, the best vibration-absorbing properties, has vulcanizate PB-5, including 24.0 phr PNB.

### 3.5. Dielectric Properties

It should be noted that rail fastener spacers are used to prevent electrical current passing from traveling to adjacent rails. In this regard, we have studied the effect of PNB on the dielectric properties of vulcanizates. In the course of studying the dielectric properties, the dependences of the capacitance ( $C$ ), specific bulk electrical resistance ( $\rho_V$ ), and the dielectric loss tangent ( $\tan\delta$ ) on temperature were obtained. Figures 6–8 show the temperature dependence curves of these indicators.

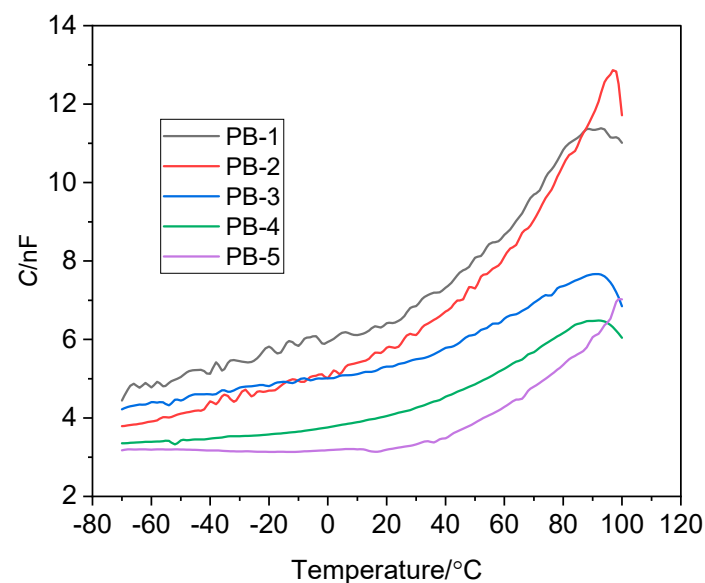
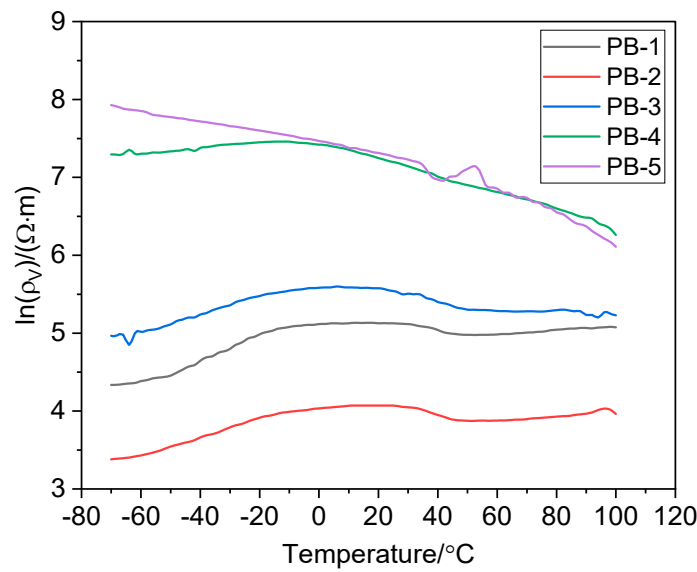
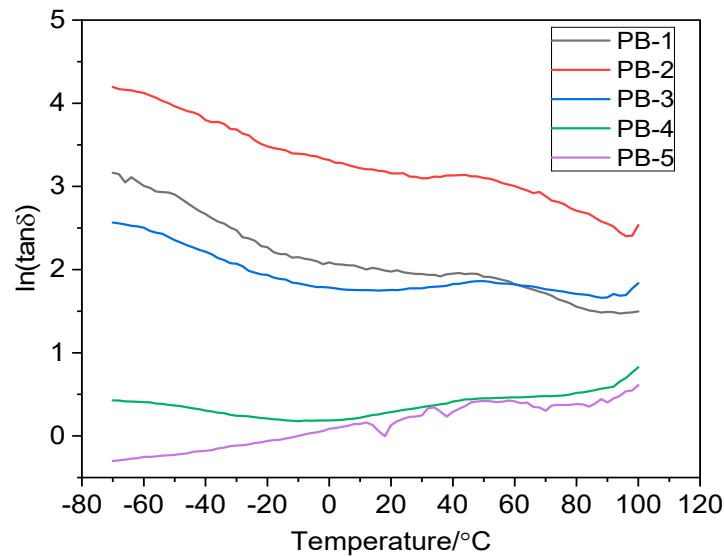


Figure 6. Temperature dependences of capacitance for vulcanizates of various types of rubber compounds.



**Figure 7.** Temperature dependences of specific volumetric electrical resistance for rubber compound vulcanizates.



**Figure 8.** Temperature dependences of the dielectric loss tangent for vulcanizates of various types of rubber compounds.

As can be seen from the results of measurements of electrical properties (Figures 6–8), the dielectric properties and the value of the specific bulk electrical resistance depend on the concentration of the RC in the rubber compound. So, the PB-4 and PB-5 vulcanizates are distinguished by the maximum resistivity. At the same time, with increasing temperature, their specific volumetric electrical resistance decreases, while for PB1-PB3 samples, it generally increases with temperature (Figure 7). The dielectric parameters, capacitance (Figure 6), and dielectric loss tangent (Figure 8), on the contrary, are minimal for PB-4 and PB-5 samples and increase in samples with a lower concentration of RC in the rubber compound. The results of studies of the dielectric properties of vulcanizates indicate that with an increase in the concentration of PNB in the rubber mixture, the specific bulk electrical resistance increases, and the tangent of the dielectric loss angle decreases, which characterizes the energy loss on the insulation. Since the heating of the material (rail pad), in particular, is associated with energy losses in the insulation, the described dielectric properties indicate that rail fastening pads will experience less heat during operation.

### 3.6. Thermal Behavior

The thermal behavior of vulcanizates was evaluated by the TGA. Figure 9 shows the TGA curves of vulcanizates.

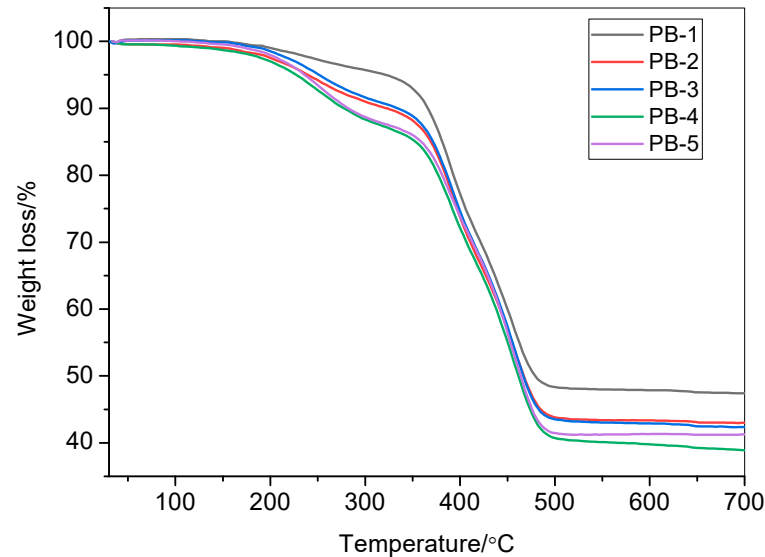


**Figure 9.** TGA curves of the investigated vulcanizates.

As can be seen from Figure 9 on the TGA curve for vulcanizates PB-1 ÷ PB-5, the onset of weight loss was observed at 150.0, 138.3, 125.3, 118.1, and 108.2 °C, respectively. The decomposition of the PB-1 vulcanizate sample occurred at 492.5 °C. For vulcanizates, PB-2 ÷ PB-5 was observed in the temperature range of 483–485 °C. It should be noted that RC-containing vulcanizates are characterized by lower thermal stability compared to PB-1 vulcanizates. Moreover, with an increase in the RC content in the rubber compound, a decrease in the thermal stability of vulcanizates from PB-1 to PB-5 is observed due to a decrease in intermolecular interaction and an increase in the mobility of rubber macromolecules, and, consequently, “loosening” of the vulcanization network. Apparently, this is due to an increase in the fraction of plasticizer Norman 747 LV contained in the RC.

## 4. Conclusions

The prospects of using PNB as a functional ingredient of directional action for a rubber compound based on a combination of isoprene,  $\alpha$ -methylstyrene-butadiene, and nitrile-butadiene rubbers, intended for the manufacture of rail fasteners are shown. It is shown that an increase in the content of RC in the rubber compound leads to a decrease in the maximum and minimum torques, as well as to an increase in the curing scorch time and optimum curing time of the rubber compound, which improves its technological properties (the processability of the rubber compound). Vulcanizates containing PNB in the composition of the RC have stable physico-mechanical properties. The results of the study of dielectric properties show that with an increase in the content of PNB in the rubber compound, an increase in the specific volumetric electrical resistance of vulcanized rubbers occurs. With increasing temperature, the specific volumetric electrical resistance decreases for samples of vulcanizates containing 45.0 and 60.0 phr RC, while for the vulcanizates of the first–third options for the rubber compound, it increases with increasing temperature. It is shown that the capacitance and dielectric loss tangent are minimal for rubber samples containing 45.0 and 60.0 phr RC and these indicators increase in samples with a lower content of RC in the composition of the rubber compound. It has been established that with an increase in the content of RC in the rubber compound, there is a decrease in the thermal stability of vulcanizates due to an increase in the mobility of rubber macromolecules and, consequently, “loosening” of the spatial vulcanization network, due to an increase in the

proportion of Norman 747 LV plasticizer, contained in the RC. It has been established by the DMA method that with an increase in the content of the RC and, consequently, PNB in the rubber compound, an improvement in the vibration-damping properties of vulcanizates was observed. Vulcanized rubber containing the composition of PNB at a mass ratio of 1:1.5 and in the amount of 60.0 phr (24.0 phr (8.98 wt. %) PNB) is characterized by stable physico-mechanical, improved vibration-absorbing properties, as well as increased dielectric characteristics. This rubber compound can be used as a base for the manufacture of rail fastening gaskets for railway tracks.

**Author Contributions:** Conceptualization, validation, E.N.E., A.G.B. and E.V.S.; methodology, E.N.E.; formal analysis, E.N.E., E.V.S., V.R.V. and A.G.B.; investigation, E.N.E., E.V.S. and V.R.V.; writing—original draft preparation E.N.E.; writing—review and editing, E.N.E. and A.G.B.; supervision, S.I.S. All authors have read and agreed to the published version of the manuscript.

**Funding:** This research received no external funding.

**Institutional Review Board Statement:** Not applicable.

**Informed Consent Statement:** Not applicable.

**Data Availability Statement:** Not applicable.

**Acknowledgments:** Dynamic mechanical analysis of the investigated vulcanizates was carried out on the equipment of the Collective Usage Center «New Materials and Resource-saving Technologies» (N.I. Lobachevsky State University of Nizhny Novgorod).

**Conflicts of Interest:** The authors declare no conflict of interest.

## References

1. Kaewunruen, S.; Ishida, M.; Marich, S. Dynamic Wheel–Rail Interaction Over Rail Squat Defects. *Acoust. Aust.* **2015**, *43*, 97–107. [[CrossRef](#)]
2. Ďungel, J.; Zvolenský, P.; Grenčík, J.; Leštinský, L.; Krivda, J. Localization of Increased Noise at Operating Speed of a Passenger Wagon. *Sustainability* **2021**, *13*, 453. [[CrossRef](#)]
3. Tavares de Freitas, R.; Kaewunruen, S. Life Cycle Cost Evaluation of Noise and Vibration Control Methods at Urban Railway Turnouts. *Environments* **2016**, *3*, 34. [[CrossRef](#)]
4. Barke, D.W.; Chiu, W.K. A Review of the Effects of Out-Of-Round Wheels on Track and Vehicle Components. *Proc. Inst. Mech. Eng. Part F J. Rail Rapid Transit* **2005**, *219*, 151–175. [[CrossRef](#)]
5. Kouroussis, G.; Connolly, D.P.; Vogiatzis, K.; Verlinden, O. Modelling the Environmental Effects of Railway Vibrations from Different Types of Rolling Stock: A Numerical Study. *Shock Vib.* **2015**, *2015*, 142807. [[CrossRef](#)]
6. Chiacchiari, L.; Loprencipe, G. Measurement methods and analysis tools for rail irregularities: A case study for urban tram track. *J. Mod. Transp.* **2015**, *23*, 137–147. [[CrossRef](#)]
7. Colaço, A.; Costa, P.A.; Connolly, D.P. The influence of train properties on railway ground vibrations. *Struct. Infrastruct. Eng.* **2015**, *12*, 517–534. [[CrossRef](#)]
8. Hao, Y.; Qi, H.; Liu, S.; Nian, V.; Zhang, Z. Study of Noise and Vibration Impacts to Buildings Due to Urban Rail Transit and Mitigation Measures. *Sustainability* **2022**, *14*, 3119. [[CrossRef](#)]
9. Mohamed, A.-M.O.; Paleologos, E.K.; Howar, F.M. Noise pollution and its impact on human health and the environment. In *Pollution Assessment for Sustainable Practices in Applied Sciences and Engineering*; Butterworth-Heinemann: Oxford, UK, 2021; pp. 975–1026. [[CrossRef](#)]
10. Michali, M.; Emrouznejad, A.; Dehnokhalaji, A.; Clegg, B. Noise-pollution efficiency analysis of European railways: A network DEA model. *Transp. Res. Part D Transp. Environ.* **2021**, *98*, 102980. [[CrossRef](#)]
11. Sahu, P.; Galhotra, A.; Raj, U.; Ranjan, R.V. A study of self-reported health problems of the people living near railway tracks in Raipur city. *J. Fam. Med. Prim. Care* **2020**, *9*, 740–744. [[CrossRef](#)]
12. Panulinova, E.; Harabinová, S.; Argalášová, L. Tram squealing noise and its impact on human health. *Noise Health* **2016**, *18*, 329–337. [[CrossRef](#)] [[PubMed](#)]
13. Demir, E.; Huang, Y.; Scholts, S.; Van Woensel, T. A selected review on the negative externalities of the freight transportation: Modeling and pricing. *Transp. Res. Part E Logist. Transp. Rev.* **2015**, *77*, 95–114. [[CrossRef](#)]
14. Elmenhorst, E.-M.; Pennig, S.; Rolny, V.; Quehl, J.; Mueller, U.; Maaß, H.; Basner, M. Examining nocturnal railway noise and aircraft noise in the field: Sleep, psychomotor performance, and annoyance. *Sci. Total Environ.* **2012**, *424*, 48–56. [[CrossRef](#)] [[PubMed](#)]
15. Wu, B.; Chen, G.; Lv, J.; Zhu, Q.; Kang, X. Generation mechanism and remedy method of rail corrugation at a sharp curved metro track with Vanguard fasteners. *J. Low Freq. Noise Vib. Act. Control* **2019**, *39*, 368–381. [[CrossRef](#)]

16. Liu, L.; Zuo, Z.; Zhou, Y.; Qin, J. Insights into the Effect of WJ-7 Fastener Rubber Pad to Vehicle-Rail-Viaduct Coupled Dynamics. *Appl. Sci.* **2020**, *10*, 1889. [[CrossRef](#)]
17. Huang, Y.; Wang, J.; Le, W.; Zhang, L.; Su, J. Study on mechanical behaviours of rail fasteners and effects on seismic performance of urban rail viaduct. *Structures* **2021**, *33*, 3822–3834. [[CrossRef](#)]
18. Liu, W.; Zhang, H.; Liu, W.; Thompson, D.J. Experimental study of the treatment measures for rail corrugation on tracks with Egg fasteners in the Beijing metro. *Proc. Inst. Mech. Eng. Part F J. Rail Rapid Transit* **2017**, *232*, 1360–1374. [[CrossRef](#)]
19. Xu, J.; Wang, K.; Liang, X.; Gao, Y.; Liu, Z.; Chen, R.; Wang, P.; Xu, F.; Wei, K. Influence of viscoelastic mechanical properties of rail pads on wheel and corrugated rail rolling contact at high speeds. *Tribol. Int.* **2020**, *151*, 106523. [[CrossRef](#)]
20. Zhang, J.; Wang, L.; Zhao, Y. Fabrication of novel hindered phenol/phenol resin/nitrile butadiene rubber hybrids and their long-period damping properties. *Polym. Compos.* **2012**, *33*, 2125–2133. [[CrossRef](#)]
21. Roche, N.; Ichchou, M.N.; Salvia, M.; Chettah, A. Dynamic Damping Properties of Thermoplastic Elastomers Based on EVA and Recycled Ground Tire Rubber. *J. Elastomers Plast.* **2011**, *43*, 317–340. [[CrossRef](#)]
22. Wang, Y.; Cao, R.; Wang, M.; Liu, X.; Zhao, X.; Lu, Y.; Feng, A.; Zhang, L. Design and synthesis of phenyl silicone rubber with functional epoxy groups through anionic copolymerization and subsequent epoxidation. *Polymer* **2020**, *186*, 122077. [[CrossRef](#)]
23. Sheng, Z.; Yang, S.; Wang, J.; Lu, Y.; Tang, K.; Song, S. Preparation and Properties Analysis of Chlorinated Butyl Rubber (CIIR)/Organic Diatomite Damping Composites. *Materials* **2018**, *11*, 2172. [[CrossRef](#)] [[PubMed](#)]
24. Zhou, X.Q.; Yu, D.Y.; Shao, X.Y.; Zhang, S.Q.; Wang, S. Research and applications of viscoelastic vibration damping materials: A review. *Compos. Struct.* **2016**, *136*, 460–480. [[CrossRef](#)]
25. Bielawski, C.W.; Benitez, D.; Morita, T.; Grubbs, R.H. Synthesis of End-Functionalized Poly(norbornene)s via Ring-Opening Metathesis Polymerization. *Macromolecules* **2001**, *34*, 8610–8618. [[CrossRef](#)]
26. Frenzel, U.; Nuyken, O. Ruthenium-based metathesis initiators: Development and use in ring-opening metathesis polymerization. *J. Polym. Sci. Part A Polym. Chem.* **2002**, *40*, 2895–2916. [[CrossRef](#)]
27. Delaude, L.; Demonceau, A.; Noels, A.F. Probing the Stereoselectivity of the Ruthenium-Catalyzed Ring-Opening Metathesis Polymerization of Norbornene and Norbornadiene Diesters. *Macromolecules* **2003**, *36*, 1446–1456. [[CrossRef](#)]
28. Li, L.; Gomes, P.T.; Lemos, M.A.N.D.A.; Lemos, F.; Fan, Z. Polymerisation of Norbornene Catalysed by Highly Active Tetradentate Chelated  $\alpha$ -Diimine Nickel Complexes. *Macromol. Chem. Phys.* **2011**, *212*, 367–374. [[CrossRef](#)]
29. Bogdanova, Y.G.; Dolzhikova, V.D.; Tikhonov, N.A.; Gringol'ts, M.L.; Kostina, Y.V.; Alent'ev, A.Y. The effect of trimethylsilyl substituents in the monomer unit on the energy characteristics of surfaces of polynorbornenes obtained via metathesis polymerization. *Polym. Sci. Ser. A* **2013**, *55*, 471–479. [[CrossRef](#)]
30. Bishop, J.P.; Register, R.A. The crystal-crystal transition in hydrogenated ring-opened polynorbornenes: Tacticity, crystal thickening, and alignment. *J. Polym. Sci. Part B Polym. Phys.* **2010**, *49*, 68–79. [[CrossRef](#)]
31. Leimgruber, S.; Trimmel, G. Olefin metathesis meets rubber chemistry and technology. *Monatsh. Chem.* **2015**, *146*, 1081–1097. [[CrossRef](#)]
32. Yang, Z.; Han, C.D. Synthesis of hydrogenated functional polynorbornene (HFPNB) and rheology of HFPNB-based miscible blends with hydrogen bonding. *Polymer* **2008**, *49*, 5128–5136. [[CrossRef](#)]
33. Nickel, A.; Edgecombe, B.D. Industrial Applications of ROMP. In *Polymer Science: A Comprehensive Reference*; Elsevier: Amsterdam, The Netherlands, 2012; pp. 749–759.
34. Qu, M.; Ma, Y.; Li, C.; Shi, X. Investigation of the properties of polynorbornene rubber/EPDM blends. *J. Elastomers Plast.* **2016**, *49*, 560–573. [[CrossRef](#)]
35. Kumar, N.; Singh, K.P.; Giri, A.; Singh, S.P. Transport mechanism and diffusion kinetics of kerosene through polynorbornene rubber/natural rubber blends. *Polym. Bull.* **2022**, *79*, 5305–5325. [[CrossRef](#)]
36. Yalçinkaya, E.E. Polynorbornene/MMT nanocomposites via surface-initiated ROMP: Synthesis, characterization, and dielectric and thermal properties. *J. Mater. Sci.* **2013**, *49*, 749–757. [[CrossRef](#)]
37. Xu, J.; Li, A.; Wang, H.; Shen, Y. Dynamic mechanical analysis of Norsorex/acrylonitrile butadiene rubber blends and their application in vibration control of steel frames. *Adv. Mech. Eng.* **2016**, *8*, 1687814016662561. [[CrossRef](#)]
38. Flory, P.J.; Rehner, J. Statistical Mechanics of Cross-Linked Polymer Networks I. Rubberlike Elasticity. *J. Chem. Phys.* **1943**, *11*, 512–520. [[CrossRef](#)]
39. Kim, D.Y.; Park, J.W.; Lee, D.Y.; Seo, K.H. Correlation between the Crosslink Characteristics and Mechanical Properties of Natural Rubber Compound via Accelerators and Reinforcement. *Polymers* **2020**, *12*, 2020. [[CrossRef](#)]
40. Mohamad Aini, N.; Othman, N.; Hussin, M.; Sahakaro, K.; Hayeemasae, N. Hydroxymethylation-Modified Lignin and Its Effectiveness as a Filler in Rubber Composites. *Processes* **2019**, *7*, 315. [[CrossRef](#)]
41. Pongdong, W.; Nakason, C.; Kummerlöwe, C.; Vennemann, N. Influence of filler from a renewable resource and silane coupling agent on the properties of epoxidized natural rubber vulcanizates. *J. Chem.* **2015**, *2015*, 796459. [[CrossRef](#)]
42. Zeng, W.; Du, Y.; Xue, Y.; Frisch, H.L. Solubility Parameters. In *Physical Properties of Polymers Handbook*; Mark, J.E., Ed.; Springer: New York, NY, USA, 2007; pp. 289–303. [[CrossRef](#)]
43. van Krevelen, D.W.; Nijenhuis, K.T. Properties of Polymers. In *Their Correlation with Chemical Structure; Their Numerical Estimation and Prediction from Additive Group Contributions*; Elsevier: Amsterdam, The Netherlands, 2009; 1004p.

44. Gronski, W.; Hoffmann, U.; Simon, G.; Wutzler, A.; Straube, E. Structure and Density of Crosslinks in Natural-Rubber Vulcanizates. A Combined Analysis by NMR Spectroscopy, Mechanical Measurements, and Rubber-Elastic Theory. *Rubber Chem. Technol.* **1992**, *65*, 63–77. [[CrossRef](#)]
45. Marzocca, A.J.; Rodríguez Garraza, A.L.; Mansilla, M.A. Evaluation of the polymer–solvent interaction parameter  $\chi$  for the system cured polybutadiene rubber and toluene. *Polym. Test.* **2010**, *29*, 119–126. [[CrossRef](#)]
46. Sae-oui, P.; Sirisinha, C.; Wantana, T.; Hatthapanit, K. Influence of silica loading on the mechanical properties and resistance to oil and thermal aging of CR/NR blends. *J. Appl. Polym. Sci.* **2007**, *104*, 3478–3483. [[CrossRef](#)]
47. Mansilla, M.A.; Marzocca, A.J.; Macchi, C.; Somoza, A. Influence of vulcanization temperature on the cure kinetics and on the microstructural properties in natural rubber/styrene-butadiene rubber blends prepared by solution mixing. *Eur. Polym. J.* **2015**, *69*, 50–61. [[CrossRef](#)]
48. Ago, M.; Jakes, J.E.; Rojas, O.J. Thermomechanical Properties of Lignin-Based Electrospun Nanofibers and Films Reinforced with Cellulose Nanocrystals: A Dynamic Mechanical and Nanoindentation Study. *ACS Appl. Mater. Interfaces* **2013**, *5*, 11768–11776. [[CrossRef](#)] [[PubMed](#)]
49. Lu, Y.C.; Shinozaki, D.M. Temperature Dependent Viscoelastic Properties of Polymers Investigated by Small-Scale Dynamic Mechanical Analysis. *Exp. Mech.* **2010**, *50*, 71–77. [[CrossRef](#)]
50. Moradi, G.; Nassiri, P.; Ershad-Langroudi, A.; Monazzam, M.R. Acoustical, damping and thermal properties of polyurethane/poly(methyl methacrylate)-based semi-interpenetrating polymer network foams. *Plast. Rubber Compos.* **2018**, *47*, 221–231. [[CrossRef](#)]
51. Kablov, E.N.; Sagomonova, V.A.; Sorokin, A.E.; Tselikin, V.V.; Gulyaev, A.I. A Study of the Structure and Properties of Polymer Composite Materials with Integrated Vibration Absorbing Layer. *Polym. Sci. Ser. D* **2020**, *13*, 335–340. [[CrossRef](#)]
52. Egorov, E.N.; Ushmarin, N.F.; Sandalov, S.I.; Kol'tsov, N.I. Research of operational and dynamic properties of rubber for products working in sea water. *ChemChemTech Izv. Vyssh. Uchebn. Zaved. Khim. Khim. Tekhnol.* **2020**, *63*, 96–102. [[CrossRef](#)]
53. Egorov, E.N.; Ushmarin, N.F.; Sandalov, S.I.; Kol'tsov, N.I.; Voronchikhin, V.D. Investigation of the dynamic properties of seawater-resistant rubber. *J. Sib. Fed. Univ. Chem.* **2021**, *14*, 38–44. [[CrossRef](#)]
54. Ushmarin, N.F.; Egorov, E.N.; Grigor'ev, V.S.; Sandalov, S.I.; Kol'tsov, N.I. Influence of Chlorobutyl Caoutchouc on the Dynamic Properties of a Rubber Based on General-Purpose Caoutchoucs. *Russ. J. Gen. Chem.* **2022**, *92*, 1862–1865. [[CrossRef](#)]
55. Sharifi, M.J.; Ghalekhondabi, V.; Fazlali, A. Investigation of the underwater sound absorption and damping properties of polyurethane elastomer. *J. Therm. Anal. Calorim.* **2022**, *147*, 4113–4118. [[CrossRef](#)]

**Disclaimer/Publisher's Note:** The statements, opinions and data contained in all publications are solely those of the individual author(s) and contributor(s) and not of MDPI and/or the editor(s). MDPI and/or the editor(s) disclaim responsibility for any injury to people or property resulting from any ideas, methods, instructions or products referred to in the content.